Sea, Sails and Foils: Using a CFD-based Dynamic VPP to Assess Racing Sailing Yachts' Performance in Waves

Pierre Robin, Alban Leroyer, David de Prémorel, Jeroen Wackers

THE 25TH CHESAPEAKE SAILING YACHT SYMPOSIUM
ANNAPOLIS, MARYLAND, MARCH 2025

Sea, Sails and Foils: Using a CFD-based Dynamic VPP to Assess Racing Sailing Yachts' Performance in Waves

Pierre Robin
Nantes Université, École Centrale Nantes, CNRS, LHEEA, UMR 6598, F-44000 Nantes, France
Finot-Conq Architectes Navals, France, pierre.robin@ec-nantes.fr.

Alban Leroyer
Nantes Université, École Centrale Nantes, CNRS, LHEEA, UMR 6598, F-44000 Nantes,France.

David de Prémorel
Finot-Conq Architectes Navals, France.

Jeroen Wackers
Nantes Université, École Centrale Nantes, CNRS, LHEEA, UMR 6598, F-44000 Nantes,France.

Abstract. In this paper, we present new developments and improvements made to a Computational Fluid Dynamics (CFD)-based Dynamic Velocity Prediction Program (DVPP) for predicting sailing yacht performance in waves. The DVPP and its use for computing equilibrium states and predicting the optimal speed of a yacht design were detailed in a previous paper. The enhancements introduced here aim to help naval architects evaluate their designs in more realistic offshore racing conditions. First, waves modelling has been improved and a PID-controlled rudder enabling six degrees of freedom (DoF) simulations can now be used for course control. The computation of aerodynamic forces has been refined to include the effects of added mass. Finally, the sock-mesh approach has been expanded to simulate a fully appended yacht, incorporating foil fluid-structure interaction through a pragmatic method.

Keywords: CFD; VPP; sailing; hydrofoil; waves; FSI.

NOMENCLATURE

C_{sail}	Aerodynamic coefficient (Force or Torque) [-]
c	Foil chord [m]
c_s	Sailplan chord [m]
e	Bearing angle error [deg]
E	Sail foot [m]
$\tilde{E}$	First elliptic integral [-]
f	Boom height [m]
G_{max}	Limitation factor of modal weighting coefficient gradient [m^{-1}]
$H_{1/3}$	Wave significant height [m]
$J_{a,xx}$, $J_{a,yy}$	Sail added mass inertia moment around x-axis and y-axis [N.m]
k	Elliptic modulus [-]
$\tilde{K}$	Second elliptic integral [-]
K_d, K_i, K_p	Derivative, Integral and Proportional Gains [-]
K_r	Windward rudder coefficient [-]

$M_{a,xx}$, $M_{a,yy}$	Sail added mass moment around x-axis and y-axis [N.m]
P	Sail leech [m]
P_{ow}	Sail power parameter [-]
Re	Reynolds number [-]
S	Reduction factor for added inertia [-]
S_a	Adimensional factor for modal weighting coefficient gradient [-]
S_e	Ellipse area [m^2]
T_r	Period of rudder angle actualization [s]
T_w	Wave period [s]
V_B	Yacht's speed [kn]
$V_{B,init}$	Initial yacht's speed [kn]
V_t	True Wind Speed [kn]
V_a	Apparent Wind Speed [kn]
w	Modal weight coefficient [-]
$y^+, y^+_{\max}, y^+_{\min}$	Wall distance, Maximal value of wall distance, Minimal value of wall distance [-]
$z_{max,sailplan}$	Maximal height of sailplan
β_a	Apparent Wind Angle [deg]
β_t	True Wind Angle [deg]
γ	Yacht's Leeway Angle [deg]
$\delta_l, \delta_w, \delta_{max}$	Leeward and Windward Rudder Angle, Maximal Rudder Angle [deg]
λ_k^i	RBF weight coefficients [-]
λ_s	Taper ratio of mainsail [-]
ν	Fluid Dynamic Viscosity [$kg.m^{-1}s^{-1}$]
ϕ	Yacht's Heel angle [deg]
ρ	Fluid Density [$kg.m^{-3}$]
φ	Radial-Basis Function [-]
θ, $\ddot{\theta}$	Yacht's Pitch Angle [deg], Yacht's Pitch Angular Acceleration [$deg.s^{-2}$]
AGR	Adaptive Grid Refinement
AWA	Apparent Wind Angle
AWS	Apparent Wind Speed
CFD	Computational Fluid Dynamics
CPU	Central Processing Unit
DoF	Degree of Freedom
FSI	Fluid-Structure Interaction
FS-PH	Free-Surface and Pressure Hessian
IMOCA	International Monohull Open Class Association
MS-FCH	Multi-Surface and Flux-Component Hessian
TWA	True Wind Angle
TWS	True Wind Speed
VPP	Velocity Prediction Program

1 INTRODUCTION

Whether it is from videos captured in Southern oceans during the Ocean Race or from data gathered during the 2020-2021 edition of the Vendée Globe, it has become clear that modern yachts' (and especially IMOCAs) performance in waves is crucial to win offshore races, especially around-the-world races. Many skippers have also expressed their need for more comfort while sailing through rough seas. This raises the need for a numerical tool able to simulate these foil-equipped yachts in realistic sea states to help naval architects designing IMOCAs that are better tailored to operating in waves.

System-based VPP are the classical tools used by naval architects to assess and compare their designs' performance. These tools essentially compute the equilibrium of the forces applied to the yacht using Newton's second law, and output a polar containing optimal yacht speeds and state variables (leeway angle, heel angle, sailplan configuration, etc.) for an extended range of True Wind Angle (TWA) and True Wind Speed (TWS). If some VPPs still rely on analytical formulas for hydrodynamics (ORC, 2021), more recent ones perform interpolation in a matrix of the hydrodynamic forces. If this matrix was previously obtained with towing tank trials, it is now often computed using CFD simulations in 80 to 200 configurations (with different combinations of pitch, trim, draft, heel, speed, etc.). When using this approach, any change in the hull design means that a new matrix should be computed, since the hydrodynamic forces applied on the yacht are likely to be different. Thus, traditional VPPs, while very efficient at optimizing settings and configurations for a given design, are somewhat impractical for hull-shape optimization.

The last few years saw the advent of system-based programs designed to dynamically simulate a yacht, and for some of them to do it in real-time. The limitations of using steady simulations to optimize an offshore racing sailing yacht which operates in highly unsteady environments were already discussed in Kerdraon (2021). In the latter, a system-based 6DOF Dynamic Velocity Prediction Program is presented. Appendage forces are modelled using an unsteady lifting line method, aerodynamic forces are obtained from interpolation in aerodynamic data matrices and waves are integrated as additional forces directly in the hydrodynamic loads. The described program can either be run as a VPP or as a real-time simulator. Similarly, in the industry, the widely used Meta and Gomboc are also system-based Dynamic Velocity Prediction Programs that support these two applications. However, to the authors' knowledge, no documentation or publications on these software tools are publicly available. In a different field, but for the same purpose, Kjellberg et al. (2023) presented a system-based 6-DOF VPP including the modelling of a seaway and unsteady aerodynamics, which relies on a potential method for the hydrodynamics while the aerodynamics are computed using a lifting line method. When using system-based VPP, forces applied on the yacht's hull and its different components (sails, foils, rudders, etc.) are modelled separately, thus interactions between them must be approximated at best, if not neglected entirely.

This makes CFD-based VPP an interesting alternative to assess sailing yachts performance. Here, the fully-appended yacht is modelled in the CFD software, aerodynamic forces are directly applied to the boat during the CFD computation, while the hydrodynamics RANS flow solver handles the hydrodynamic forces and the motions of the yacht. This approach results in dynamic changes in all degrees of freedom (DoF), such as trim, sinkage, heel, etc, leading to a coupling between aerodynamic and hydrodynamic effects. In Roux et al. (2008) 5-DoF simulations using a coupling between a CFD code solving hydrodynamics and a potential-flow code computing aerodynamic forces are presented and applied to an AC90 yacht. This proved the feasibility and the interest of an aerodynamic force input to a hydrodynamic CFD solver. Later, Böhm (2014), Lindstrand Levin and Larsson (2017) and Persson et al. (2021) also presented VPP programs using RANS CFD solvers to compute hydrodynamic forces and body motions, but with aerodynamics relying on analytical models. All three VPP programs were successfully applied to a range of boats including a Laser dinghy (Lindstrand Levin and Larsson, 2017), an AC90 yacht (Böhm, 2014), and the Sailing Yacht Research Foundation (SYRF)

yacht (Persson et al., 2021). However, none of these works were explicitly developed with a focus on accommodating foil-equipped yachts or addressing ship-in-wave performance. Their primary objective was to find equilibrium states and optimize yacht speed, similar to the approach of a conventional static VPP.

This lead us to investigate a CFD-based Dynamic VPP integrated in the CFD code FINE/Marine. This tool can both be used to find the optimal yacht's speed through a search of equilibrium states in a few keywind sailing conditions as well as to simulate a yacht sailing in waves. With respect to (Robin et al., 2024) which mainly concerns the first use of our VPP, developments have progressed and our tool now allows to assess the performance of racing sailing yachts in unsteady conditions. This paper will hence focus on the different improvements brought to it regrouped here in three categories, namely the Sea state which requires appropriate meshing and rudder control, Sails for which the unsteady aerodynamics are modelled, and Foils with fluid-structure interaction.

2 NUMERICAL TOOLS

Our DVPP uses FINE/Marine which is a marine-oriented computing suite, distributed by Cadence Design Systems (formerly Numeca International) and used by many naval architects for various hydrodynamics applications. The suite features the unstructured hexahedral mesher Hexpress, as well as the flow solver ISIS-CFD, which has extensive capabilities to connect external modules. The finotconq VPP is one of those modules.

2.1 ISIS-CFD

The flow solver ISIS-CFD is an incompressible unsteady Navier-Stokes equations solver with various Reynold-Averaged Navier Stokes (RANS) or RANS/Large Eddy Simulation hybrid turbulence models for multi-fluid flows which is developed by the METHRIC team of the LHEEA Laboratory.

The solver features a mixture-fluid formulation to model the water-air interface (Queutey and Visonneau, 2007; Wackers et al., 2011). The flow equations are discretized in a finite-volume framework, using pressure-velocity coupling obtained through implicit time integration with a Rhie & Chow SIMPLE-type method. The discretization is face-based. While all unknown state variables are cell-centred, the systems of equations used in the implicit time stepping procedure are constructed face by face. This technique poses no specific requirements on the topology of the cells. Therefore, the grids can be completely unstructured, and cells with an arbitrary number of arbitrarily-shaped faces are accepted. The AVLSMART scheme (Pržulj and Basara, 2001) is used for all convective fluxes, except for the volume fraction which uses the compressive BRICS scheme (Wackers et al., 2011). Diffusive terms are represented with central differences. The software suite has been extensively tested for different types of simulations. Examples of tests can be found in Deng et al., 2015 for cargo ships, and Prince and Claughton, 2016 for sailing yachts.

All calculations presented in this paper used RANS equations and the $k-\omega$ SST turbulence model with wall functions. The y+ of the first viscous layer is chosen for each computation, dependent on the Reynolds number of the yacht. Following FINE/Marine best practices, this choice is made as:

$$y^+ = \max\left(y^+_{\min}, \min\left(30 + \frac{270\,(Re - 10^6)}{10^9}, y^+_{\max}\right)\right), \tag{1}$$

with $y^+_{\max} = 300$, $y^+_{\min} = 50$ and Re the Reynolds number.

2.2 Computing Yacht Motions

For 5 or 6-DoF VPP computations, a coupling between the flow, the external forces and yacht motions is necessary as the motion of the yacht modifies the flow, and as the flow applies forces on the yacht, modifying its kinematics.

Thus, ISIS-CFD uses non-linear iterations inside each single time step to solve both the Navier-Stokes equations and the yacht's dynamics at the same time and perform the coupling between flow and body motion (Leroyer and Visonneau, 2005). For every non-linear iteration the motions of the yacht are updated, the mesh is deformed accordingly and the flow is solved. Forces and moments applied on the yacht can then be computed using the newly obtained flow before a new non-linear iteration starts.

To handle large motions of bodies, ISIS-CFD relies on an overset method, with a finely meshed domain around the body overlapping a background domain and moving through it. These two domains are dynamically coupled using interpolation, either through a least squares approach or with a weighted distance scheme. As VPP simulations induce major changes in the yacht's attitude, whether it is from sail power changes that lead to heeling or from sailing in waves, the use of overset grids has become a must-have. When simulating an IMOCA and all its appendages in the VPP, up to 4 overset domains are used: the hull and the keel are included in the yacht overset domain (blue in Fig.1) which also contains two rudder overset domains (in red), as well as the sock-mesh overset domain for the foil (in yellow).

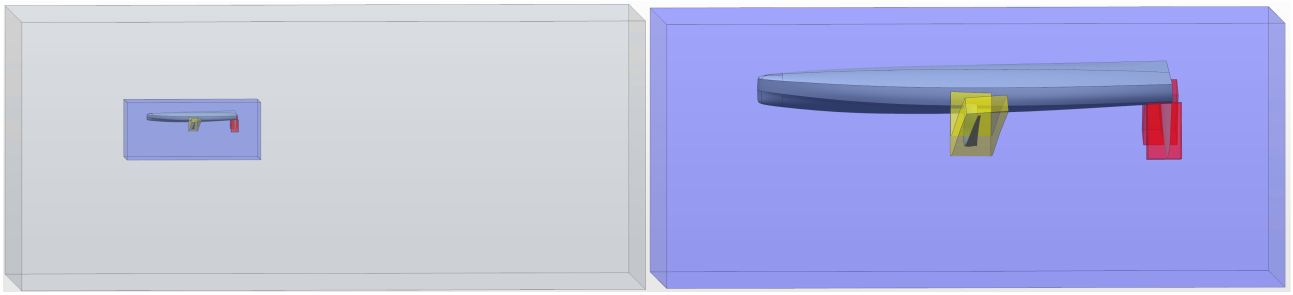

(a) Global view **(b)** Detailed view of the boat overset domain

Figure 1. Use of overset domains for a typical IMOCA VPP simulation.

2.3 Adaptive Grid Refinement and Sock-mesh Approach

FINE/Marine contains an adaptive grid refinement (AGR) algorithm, with several available criteria that allow the mesh to be automatically refined locally, during the computation (Wackers et al., 2017). Mesh adaptation enhances the capturing of flow details, either for waves, wake flows, or in boundary layers around bodies, especially around hydrofoil edges. This increases the accuracy of the computed forces for a given mesh size (Wackers et al., 2022).

When a good accuracy for the forces applied on bodies as well as a good understanding of the flow in the boundary layer are needed (which is typically the case in calculations involving hydrofoils) the Multi-Surface and Flux-Component Hessian (MS-FCH) criterion is preferred to pilot the mesh adaptation (Wackers et al., 2022). With this criterion, the refinement is based not only on the free-surface position but also on the Hessian of both pressure and velocity. Calculations using the MS-FCH criterion allow users to generate a coarse initial mesh on bodies, and to leave local mesh refinements to the AGR. Furthermore, the benefits of using the MS-FCH criterion are reinforced when using the sock-mesh approach described in Robin et al. (2022), which aligns the meshes with curved hydrofoils.

2.4 The finot-conq VPP

Our dynamic CFD-based VPP is integrated in FINE/Marine and its use to find equilibrium states and optimize boat speed V_B on flat waters was extensively covered in Robin et al. (2024).

The general process of the VPP to simulate a yacht sailing in a seaway is described in Fig. 2. The VPP is a module added to FINE/Marine, thus its use requires first to set up a classical FINE/Marine computation. Additionally, the VPP module requires the user to provide a True Wind Angle (TWA) β_t, a True Wind Speed (TWS) V_t and some of the yacht's main characteristics. For example, length over all (LOA), freeboard height air draft, etc. are required to compute windage forces.

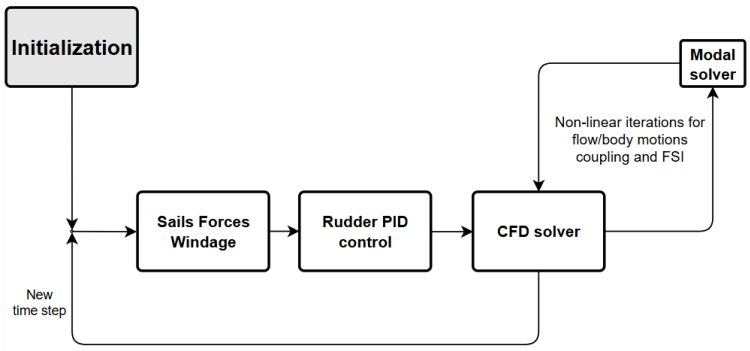

Figure 2. VPP code general process.

Once this data is read and FINE/Marine has started, the VPP code computes sails and windage forces (Section 4). The PID-controller then compares the current course of the yacht to the desired setpoint and updates the rudder angle (Section 3.2) if needed. The resulting forces and moments are input to the flow solver ISIS-CFD, which solves the flow and the motions of the yacht and handles the deformation of the foil using an internal modal solver (Section 5).

3 SEA STATE

The study of sea state effects on sailing yachts requires an accurate modelling of the waves and their interactions with the yacht. This section covers advancements in AGR adapted to wave modelling, as well as control strategies for rudder handling during ship-in-waves simulations. Both these approaches aim to enhance the fidelity of the ship-in-waves VPP simulations and to assess sailing yacht performance in more realistic sea conditions.

3.1 Adaptive Grid Refinement for Waves Modelling

For ship-in-waves simulations using AGR, the current FINE/Marine state of the art is to use the Free-Surface and Pressure Hessian (FS-PH), which is a combined criterion based on the free-surface and the Hessian of the pressure (Wackers et al., 2014). This criterion is combined with an initial mesh that is already refined around the free-surface. On the other hand, the MS-FCH criterion has proven very useful for sailing yachts or foil-only simulations in calm water (Wackers et al., 2022, Robin et al., 2022) since it allows for a coarse initial mesh, which only requires that geometrical details are captured. Hence, efforts were made to extend the use of the MS-FCH AGR criterion with coarse initial meshes to seakeeping simulations, similarly to already defined guidelines for ship resistance studies (Wackers et al., 2022) or hydrofoil simulations (Richeux, 2022).

Abgrall (2024) presents a comparison of refined meshes obtained with two protocols, one using a slightly modified MS-FCH and the other one the FS-PH criterion. Modifications brought to the MS-FCH criterion essentially consisted in changing the order of numerical operations and the methods used to compute Hessians. This comparison proved that both the FS-PH and the MS-FCH are able to refine the mesh to accurately capture the waves, but also that both criteria give very similar meshes as the contribution of the flow's velocity in the refinement decision is neglectable for cells located in the waves. Results obtained with the FS-PH protocol and with the MS-FCH with and without modifications are presented in Fig. 3. However, additional work is still needed before systematic use of MS-FCH criterion for ship-in-waves simulations can be recommended. While the first democase, an IMOCA VPP study on flat waters, presented in Section 6 uses the MS-FCH criterion, the second democase, an IMOCA yacht sailing in waves, uses the FS-PH criterion.

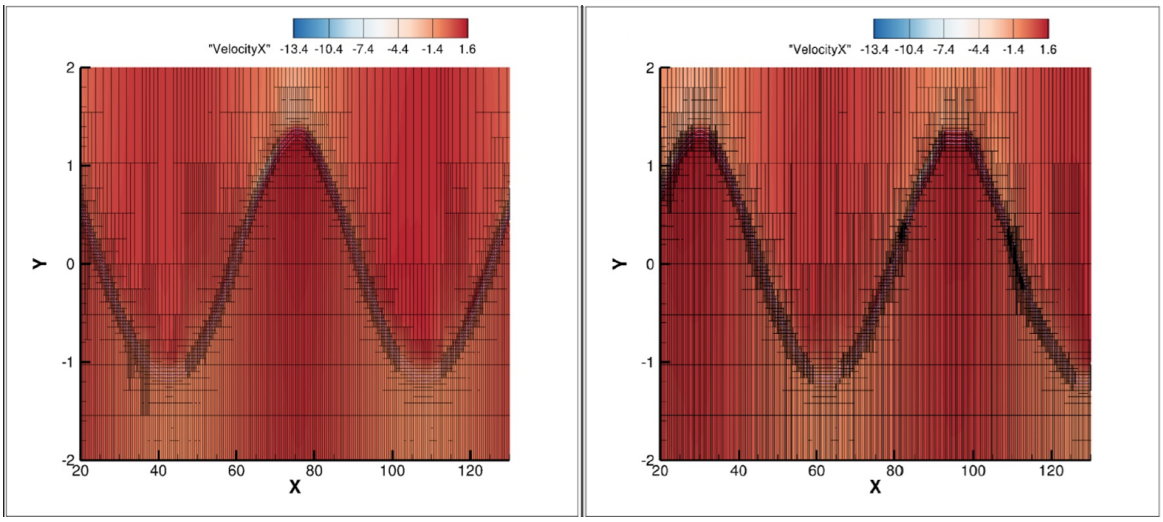

Figure 3. Comparison of the mesh obtained with FS-PH and a refined initial mesh (on the left) with the mesh obtained with MS-FCH and a coarse initial mesh (on the right)

3.2 Rudder Handling

In an effort to replicate the real behaviour of IMOCAs in waves, a PID-control of the rudder(s) has been developed. As simulations using this approach are 6-DoF, the rudder geometry needs to be included and is placed in an overset domain, as depicted in Fig. 1a.

As IMOCA class yachts typically include a twin-rudder system, the leeward rudder's angle $\delta_l(t)$ is controlled using, as error e, the difference between the yacht's course angle and a given target bearing:

$$\delta_{\mathrm{l}}(t) = K_p\, e(t) + K_i \int_{t-T_r}^{t} e(\tau)\,\mathrm{d}\tau + K_d\,\frac{\mathrm{d}e(t)}{\mathrm{d}t}. \tag{2}$$

As a simplified model of a real steering system, the windward rudder's angle is obtained from the leeward rudder angle with the following equation:

$$\delta_{\mathrm{w}}(t) = \delta_{\mathrm{l}}(t) * K_r \tag{3}$$

In the same spirit, the angular speed, the maximum angle of the rudders δ_{max} and the PID-controller frequency T_r are adjustable to mimic a real autopilot control behaviour. In the computation presented in Section 6, PID coefficient values and twin-rudder system coefficient values used were respectively $K_p = 0.5$, $K_i = 0.25$, $K_d = 0.1$ and $K_r = 1.2$. PID coefficient values were determined using previous VPP computations (not shown here) where K_p, K_i and K_d were adjusted using a trial-and-error process that aimed at maintaining $e < 5°$ during the whole simulation of an IMOCA sailing in waves and to attain the desired setpoint before 20s of physical time.

4 SAIL AERODYNAMICS

This section focuses on modelling sail aerodynamics and first exposes advancements in the interpolation of aerodynamic coefficients using Radial-Basis Functions (RBF), enhancing the flexibility and adaptability of the VPP for various propulsion systems. The section then focuses on the implementation of added mass effects in our aerodynamics model, which are essential for dynamic motion in waves. The model used is based on potential flow theory and has corrections for three-dimensionality.

4.1 Aerodynamics Coefficients Interpolation

In addition to the analytical aerodynamics coefficients based on the ORC VPP, the finot-conq VPP can use sail aerodynamics data matrices supplied by sailmakers. When these matrices are used, at each time step the code uses interpolation to determine the aerodynamic forces and moments on the sails. While the previous method of interpolation relied on cubic interpolation, we now use RBF interpolation. This aims at providing more flexibility to the process and evolutivity for any future need for more interpolation variables or to adapt to different wind propulsion systems (e.g. Flettner rotors).

The RBF formulation used is as follows. Let the aerodynamics coefficients C^k_{sail}, $(1 \leq k \leq 6)$ given in our data matrices depend on 3 variables $\mathbf{x} = [P_{ow}, \beta_a, \phi]$ (with P_{ow} is the sail power parameter, β_a the AWA, and ϕ the heeling angle) and form a dataset $\left\{\left(\mathbf{x}^k_i, C^k_i\right)\right\}_{1 \leq i \leq n_d}$ (with n_d the number of data points in the matrix), then the 6 interpolated coefficients C^k_{sail} are given by:

$$C^k_{sail}(\mathbf{x}) = \sum_{i=1}^{n_d} \lambda^k_i \, \varphi\left(\|\mathbf{x} - \mathbf{x}_i\|\right), \tag{4}$$

with λ^k_i determined so that $C^k_{sail}(\mathbf{x}^k_i) = C^k_i$. For aerodynamics data matrices interpolation, φ was chosen as $\varphi : x \to x^3$ (Forrester and Keane, 2009, Volpi et al., 2015). This kernel gives satisfying results for such data, since aerodynamic coefficients often behave like polynomials (see Fig. 4).

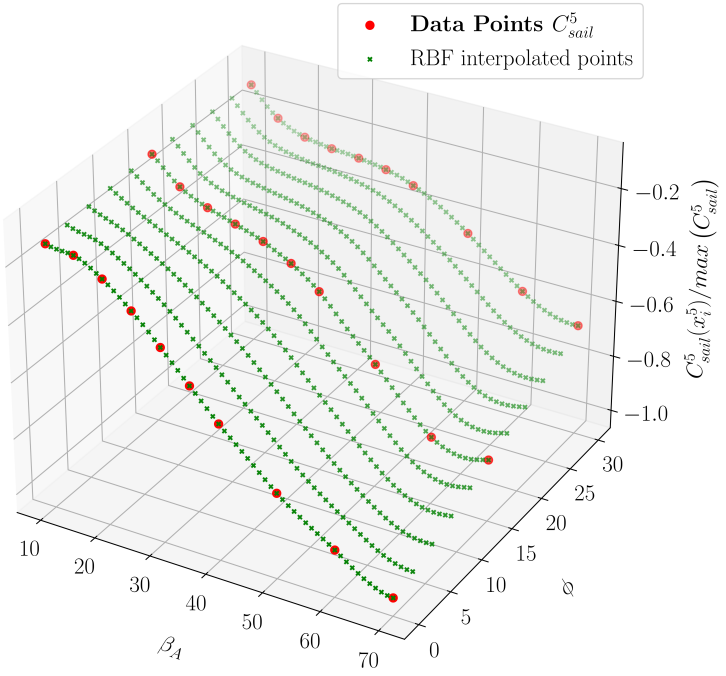

Figure 4. Interpolation obtained for sail aerodynamics coefficients describing pitch angle using RBF interpolation method. For confidentiality reasons, C^5_{sail} values have been normalized.

4.2 Added Mass Effects

Added mass refers to the additional inertia that a fluid imparts to an accelerating body, as the body must move not only itself but also the surrounding fluid. During ship-in-waves simulations, yachts usually undergo large wave-induced motions, so sail added mass effects are expected to be significant.

To account for this phenomenon, the method described in Gerhardt et al. (2009) was implemented in our VPP. Although its initial intent was to simulate tacking manoeuvres, which is not the purpose of our VPP, this method was also used recently in a system-based sailing yacht simulator and VPP (Kerdraon, 2021) together with steady-state aerodynamic coefficients determined from RANS calculations. In the method of Gerhardt et al. (2009), the sail plan is assumed to be two-dimensional and sails are assumed to be rigid. The sail plan is divided in infinitesimal strips of height dz, where z denotes the vertical coordinate, and length $c_s(z)$. Based on potential flow theory, the added mass of each strip is given by:

$$dm_a(z) = \rho_{air} \frac{\pi}{4} c_s^2(z) dz \tag{5}$$

Integrating along the whole sail plan from the height of the boom at $z = z_{boom}$ to the top of the sails at $z = z_{max,sailplan}$, gives the added moment of inertia for roll motion:

$$J_{a,xx} = \rho_{air} \frac{\pi}{4} \int_{z_{boom}}^{z_{max,sailplan}} c_s^2(z)\, dz \tag{6}$$

Gerhardt et al. (2009) also elaborated a corrective factor $S(\Lambda)$ to account for three-dimensional effects, which is given by:

$$S(\Lambda) = \frac{\pi^2 \Lambda^2 - 16}{\tilde{E}(k)(\pi^2 \Lambda^2 - 32) + 16\tilde{K}(k)} \tag{7}$$

where $\Lambda = \frac{4}{\pi}\frac{a}{b}$, with a taken as half the total height of the sail plan and b so that the area of the ellipse with semi-major axis a and semi-minor axis b S_e satisfies $S_e = \pi ab = S_{sail}$. Here, $k = \frac{a^2 - b^2}{a^2}$, while $\tilde{E}$ and $\tilde{K}$ are the complete elliptical integrals of the first and second kind respectively:

$$\begin{aligned} \tilde{E} &= \int_0^{\pi/2} \frac{1}{\sqrt{1 - k^2 sin^2\varphi}}\, d\varphi \\ \tilde{K} &= \int_0^{\pi/2} \sqrt{1 - k^2 sin^2\varphi}\, d\varphi \end{aligned} \tag{8}$$

Eventually, this yields:

$$J_{a,xx} = \rho_{air} \frac{\pi}{4} S(\Lambda) \int_{z_{boom}}^{z_{max,sailplan}} c_s^2(z)\, dz \tag{9}$$

To assess the accuracy of this method, it is compared to the added mass inertia moments obtained using ISIS-CFD. This feature of the flow solver relies on a 3-dimensional potential method to determine the added mass matrix for a given geometry (Leroyer, 2004). First, an AC90 mainsail is tested for which Gerhardt et al. (2009) gives a computed added mass inertia of $J_{a,xx} = 658 \cdot 10^3\, kg.m^2$. For ISIS-CFD, fluid properties ρ and ν were chosen as $\rho = 1.2\, kg.m^3$ and $\nu = 1.85 \cdot 10^{-5}$ which delivered

$J_{a,xx} = 754 \cdot 10^3\, kg.m^2$. Since no information is given on the AC90 mainsail deformed geometry, the sail was assumed flat which leads to no significant 3D effects.

As a second test, both methods were applied to a generic IMOCA sailplan. The geometry and the dimensions of the sails are presented in Fig. 4.2. For the IMOCA generic sailplan, Gerhardt et al. (2009)'s method gives $J_{a,xx} = 85.3 \cdot 10^3\, kg.m^2$, while ISIS-CFD yields $J_{a,xx} = 114 \cdot 10^3\, kg.m^2$. Moreover, with the latter method other coefficients, such as $J_{a,yy}$ can be obtained. For the IMOCA generic sailplan, $J_{a,yy} = 10.9 \cdot 10^3\, kg.m^2$.

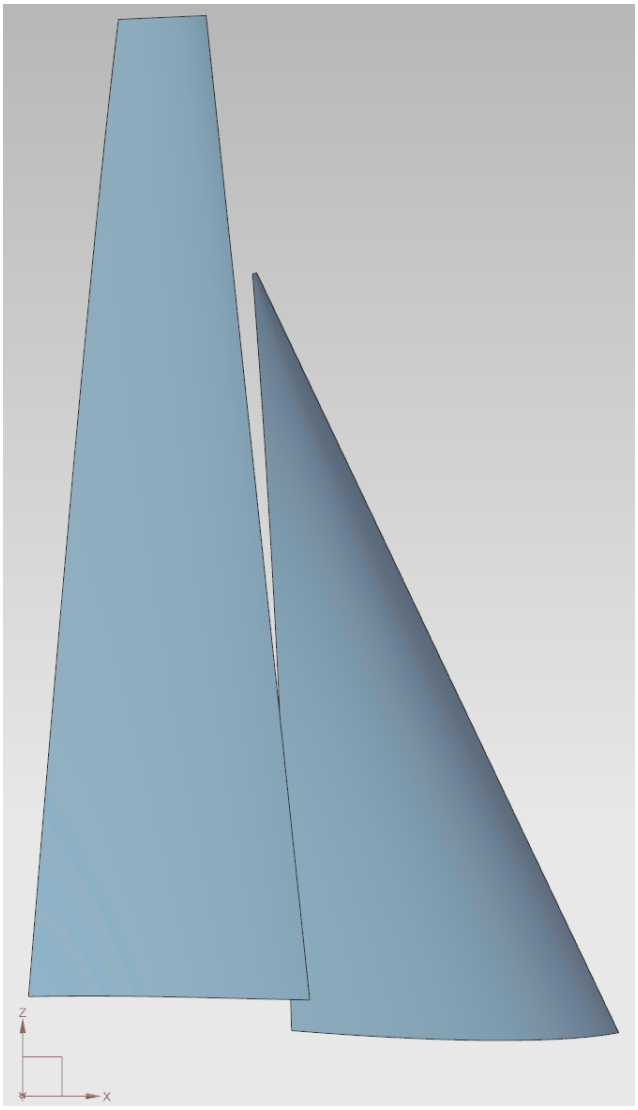

Figure 5. Generic IMOCA sailplan used for added mass comparisons.

E	P	f	λ_s
7.5	26.4	0.32	1.1

Table 1. Mainsail dimensions

E	P
8.3	18.1

Table 2. Jib dimensions

For the IMOCA sailing in waves democase computation presented in Section 6, both added inertia $J_{a,xx}$ and $J_{a,yy}$ obtained with ISIS-CFD were used, in the form of additional moments $M_{a,xx}$ and $M_{a,yy}$ input to the solver as follows:

$$\begin{aligned} M_{a,xx} &= J_{a,xx} \cdot \ddot{\phi} \\ M_{a,yy} &= J_{a,yy} \cdot \ddot{\theta} \end{aligned} \tag{10}$$

5 FOIL FSI FOR FULLY-APPENDED YACHTS USING A SOCK-MESH APPROACH

Modern hydrofoils are flexible, so it is important to take into account their deformation for performance prediction and seakeeping. We simulate foil deformation with the sock-mesh approach (Robin et al., 2022, Robin et al., 2024, Wackers et al., 2025) which encloses the foil in a slender overset domain that is easy to deform.

In this work, the sock-mesh approach has been extended to the simulation of fully-appended yachts. The hull is assumed to be fully rigid while the foil is deformable, which represents a real challenge in terms of meshing quality, especially at the vicinity of the foil/hull junction. Indeed, even very small deformations in the viscous layers of the foil can rapidly lead to negative volumes. Hence, the foil is assumed to be clamped to the hull.

In reality, IMOCA foils can deform in their casing and in the modal analysis made in a FEA solver, boundary conditions that model the real IMOCA foil bearings are used. The first deformation eigenmodes of the structure are computed in an external finite element solver and input to the flow solver. During the computation, structural deformations are obtained by computing the temporal evolution of the amplitude of these selected eigenmodes through a modal equation solved internally.(Mouton et al., 2018). Then, the deformation of the foil is pondered to obtain the following behaviour:

- The foil is fully rigid at the junction with the hull so that it stays clamped at the same location of the hull all along the computation.
- The foil is fully deformable at a certain distance from the junction with the hull.
- Between these two zones, the foil only deforms partially.

In most system-based Velocity Prediction Programs, the interaction between the hull and the foil is typically not modelled, with forces generated by each component simply aggregated. In contrast, our approach enables a detailed analysis of the foil's interaction with the hull, allowing for more comprehensive analysis. The only constraint in our method is the restriction of deformation in the vicinity of the foil/hull junction which is already very limited in practice.

To obtain the partial deformation of the foil, the modal mesh deformation procedure was modified. In ISIS-CFD, after deformations of bodies have been computed, their deformation is imposed to the mesh, weighted with a spatially varying coefficient w which goes to zero on the domain boundaries, so that the outer domain does not deform (Wackers et al., 2025). For our simulations, since the foil is included in its own mesh domain, namely the sock overset domain, only the nodes included in the sock domain undergo this regridding. First, an initial coefficient w_0 is computed as a solution of Laplace's equation with Dirichlet boundary conditions 1 on the foil surface and 0 on the part of the hull included in the sock domain (see Fig. 6). The weighting modal coefficient w then undergoes a series of operations, as it is first raised to the power q_{modal}. Then w is either clipped to extend the range of 0 and 1 with respect to coefficients w_{min} and w_{max} or linearly redistributed:

$$w \longleftarrow w^{q_{modal}}. \tag{11}$$

$$\begin{cases} w \longleftarrow 0 \quad \text{if } w^{q_{modal}} \leq w_{min}. \\ w \longleftarrow 1 \quad \text{if } w^{q_{modal}} \geq w_{max}. \\ w \longleftarrow \dfrac{w^{q_{modal}} - w_{min}}{w_{max} - w_{min}} \quad \text{otherwise.} \end{cases} \tag{12}$$

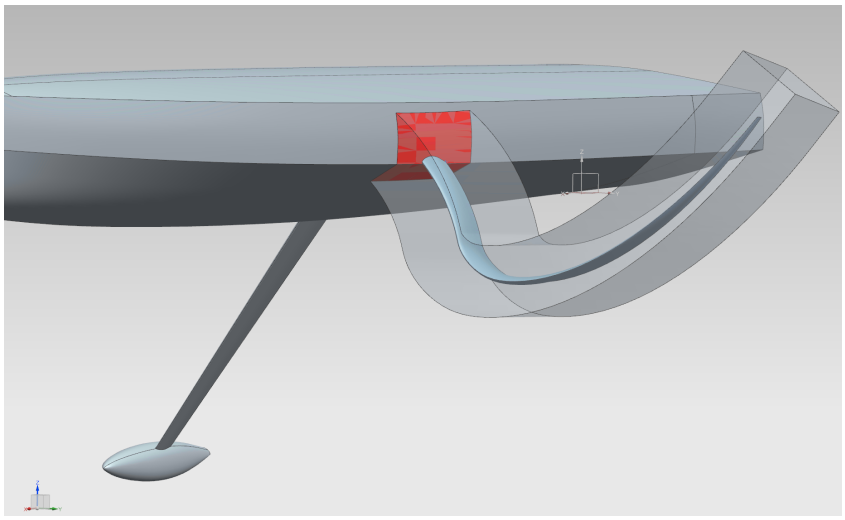

Figure 6. Hull surfaces patches included in the sock-mesh domain are highlighted in red. These patches are used in the modal weighting coefficient w process

This combination of operations (power law, clipping and linear redistribution) on w enlarges the area where $w = 0$. However, it still keeps a discontinuity in the corner joining the foil to the hull: the hull has $w = 0$ while the foil has $w = 1$. Thus, a gradient limitation-based smoothing procedure is then applied on w to remove such a discontinuity and effectively obtain $w = 1$ for every node x located at a distance from the hull surfaces patch(es). For every node in the sock domain, this second procedure imposes the gradient of w between two neighbouring cells to be inferior to G_{max}, where:

$$G_{max} = \frac{1}{S_a\, c} \tag{13}$$

with c the maximal chord of the foil and S_a a non-dimensional parameter chosen such that at a distance of $S_a * c$ from the hull patch(es), $w = 1$. The whole procedure results in an ideal transition between the rigidified part of the foil and its fully deformable part (see Fig. 7).

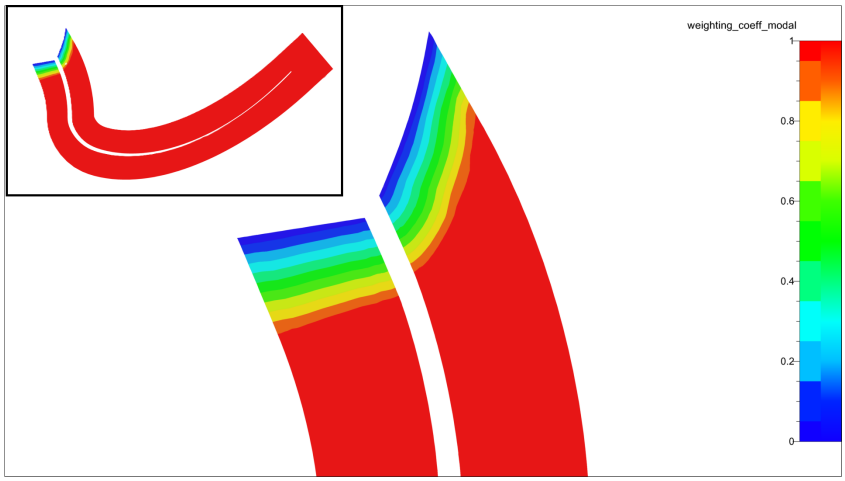

Figure 7. Modal weighting coefficients for the foil used in Section 6. Here, $w_{min} = 0.4$, $w_{max} = 0.8$, $q_{modal} = 0.7$ and $S_a = 0.5$

6 DEMOCASE

To test the dynamic VPP, it is applied to a generic IMOCA design (See Fig. 8) for two test cases, one where it sails in calm water, to show that the speed optimisation use detailed in Robin et al. (2024) is enhanced by the addition of FSI (Section 6.1), and one where it sails in waves, which includes all the new features covered in this article (Section 6.1).

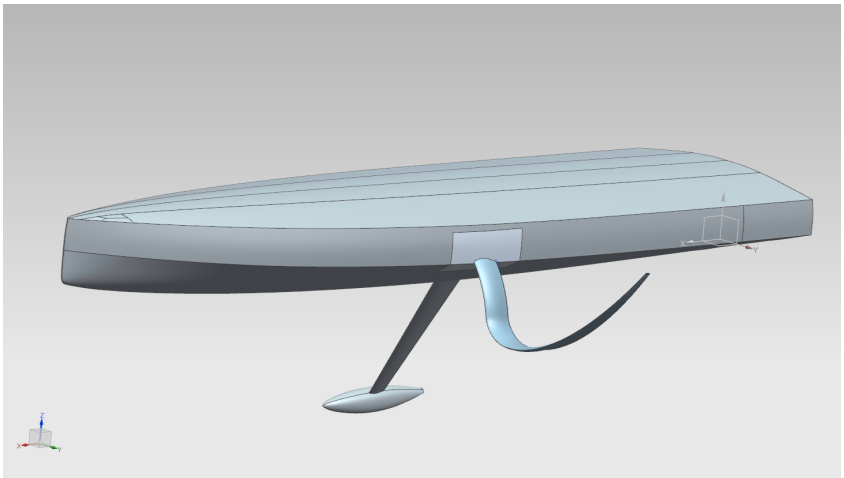

Figure 8. Geometry of the generic IMOCA design used for both democases.

6.1 VPP Use with FSI

The following calculation was made using aerodynamics data matrices, a deformable foil using the sock-mesh approach, and the analytical rudder model that balances the M_z moment induced by sails and windage with rudder forces computed from a given polar. Other parameters of the computation are listed in Tab. 3.

Table 3. Computation parameters for the upwind IMOCA simulation.

V_t [kn]	β_t [°]	Sail plan	P_{ow} range [-]
21	55	Mainsail + J2	0-0.5

The initial use of our Dynamic VPP as a way to optimize yacht's speed V_B using equilibrium states is still possible and the fidelity of the simulation is even enhanced with the use of foil's FSI. A first equilibrium has been attained and results at this stage of the computation are presented in Fig.11 and Fig.10. This single iteration of yacht's speed optimization shows that our tool can be used conjugately with a traditional static VPPs to quickly assess yacht's speed V_B, as initial conditions in which the yacht was placed in this computation were found using such tools. However, authors aim on presenting the complete 4 optimization iterations of the duet (P_{ow}, V_B) in the next version of the paper as soon as the calculation finishes. The deformed shape of the foil is presented in Fig.9 along the initial geometry. The deflection at the tip reaches 80cm which proves that the fluid-structure interaction of the foil needs to be accounted for.

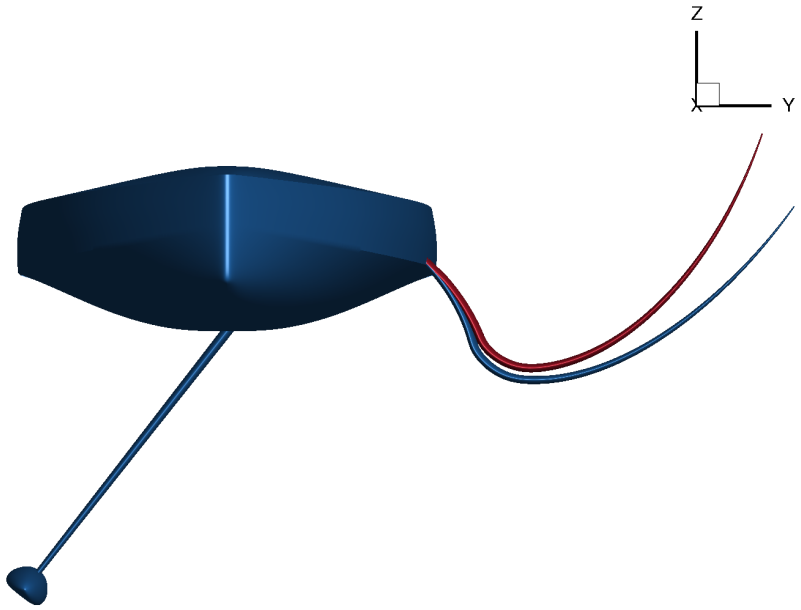

Figure 9. Deformation of the foil for the upwind case presented in Section 6. The deformed foil is represented in red.

6.2 IMOCA sailing in waves

The following calculation was made using aerodynamics data matrices with the adjunction of added mass inertia, a deformable foil using sock-mesh approach as well as the PID rudder model. The yacht is also sailing in waves of period T_w and significant height $H_{1/3}$. Other parameters of the computation are listed in Tab. 4.

Table 4. Computation parameters for the IMOCA sailing in waves simulation.

V_t [kn]	β_t [°]	Sail plan	P_{ow} range [-]	T_w[s]	$H_{1/3}$[m]
21	55	Mainsail + J2	0-0.5	7	3

This computation requires some additional work too as we are currently facing issues with the foil deformation now that the calculation is fully unsteady. We're currently investigating towards a decreasing limitation of the foil deformation during the beginning of the computation to tackle this issue. The authors hope that this democase -which uses all advanced features covered in this paper- will be ready for the next version of the paper.

7 CONCLUSIONS

The aim of this work is to develop a VPP that will allow naval architects to assess their design's performance in a various range of sea states, using higher complexity models and new developments in wave modelling, sails aerodynamics and foil's fluid-structure interaction. With the integration of our VPP in the CFD suite FINE/Marine, our VPP also beneficiate from state-of-the-art CFD techniques, such as the adaptive grid refinement or the modal approach. This paper showed through two computations that performance in waves of racing offshore sailing yachts can indeed be obtained. Moreover, the previous use of the VPP which was to optimize yacht's speed based on different equilibrium states has also been improved with the addition of foil's FSI. This leads to simulations that get one step closer to the real behaviour of IMOCAs, which indirectly facilitates the comparison with real IMOCAs' per-

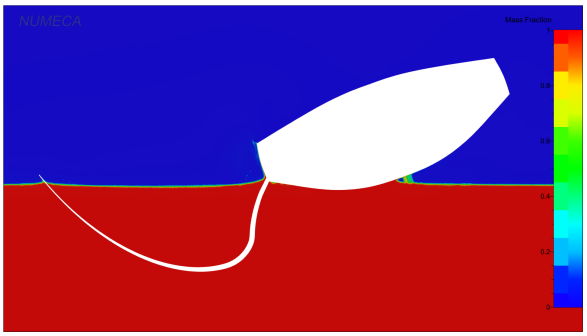

(a) Volume fraction around the yacht.

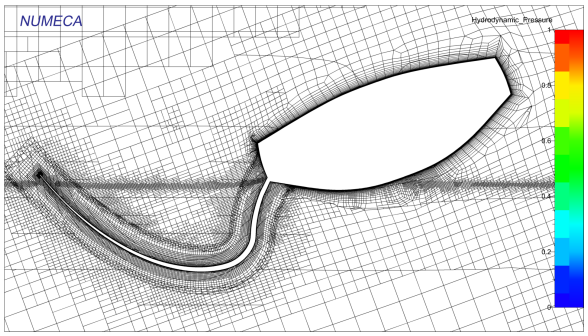

(b) Mesh around the foil.

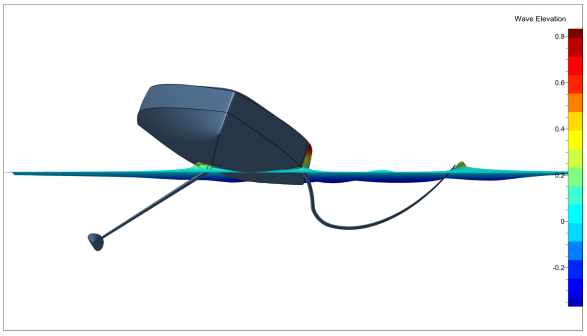

(c) Front view of the flow.

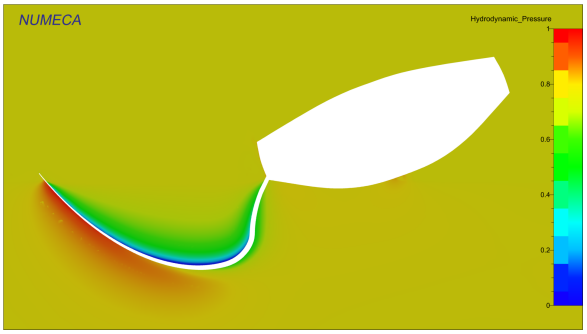

(d) Linearly redistributed hydrodynamic pressure $(P_{hydro} - P_{hydro,min}) / (P_{hydro,max} - P_{hydro,min})$ around the yacht.

Figure 10. Overview of the flow and mesh characteristics for the upwind case presented in Section 6.

formance data. Indeed, like many VPPs, results obtained with our tool are difficult to validate with experimental data. With the addition of FSI in our model, experimental setups would need to respect an additional scale for a accurate comparison.

In future works, authors hope to have access to real-life IMOCA yachts' race data and perform a comparison of the results obtained with the tool presented here to this data. The authors are currently addressing several topics in order to enhance the different models and thus the overall precision of the tool. One area for improvement lies within the aerodynamics model, as the assumed rigidity of sails can seem a strong hypothesis, especially in light winds or with large downwind sails that are likely to undergo large deformations. Another area of improvements is the foil structural model, a coupling with a beam model structural solver is currently studied. For the naval architect, the beam approach is interesting as it does not require the separate calculation step of the first deformation eigenmodes, and because the description of a foil as a beam, which is usually known, is directly input to the code. Eventually, authors would be interested in applying the tool covered in this paper to vessels that use Wind-Assisted Propulsion Systems. For the design of these ships and their appendages, our tool could be an interesting alternative to system-based VPP, for the same reasons that apply to racing sailing yachts.

ACKNOWLEDGEMENTS

The authors are especially grateful to Mr. Antoine Koch that co-designed the hull and foils of the IMOCA geometry used in this paper.

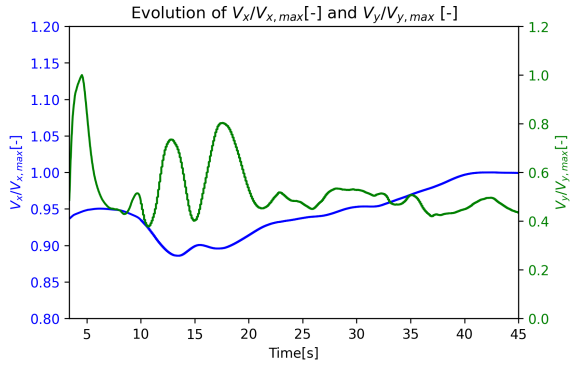

(a) Evolution of the yacht's normalized speeds along x-axis $V_x/V_{x,max}$ and y-axis $V_y/V_{y,max}$ during the computation.

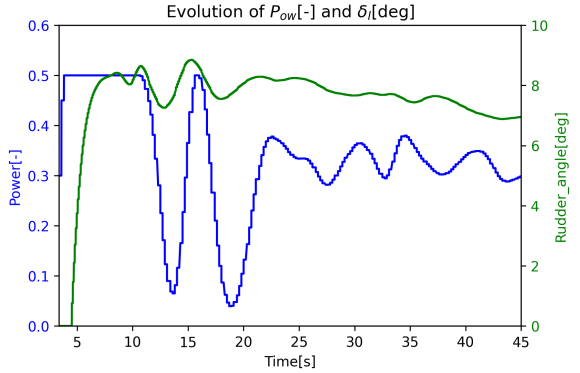

(b) Evolution of the sail power P_{ow} and rudder angle δ during the computation.

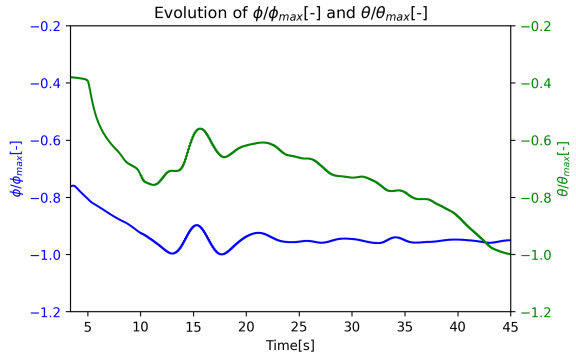

(c) Evolution of the yacht's normalized heel ϕ/ϕ_{max} and pitch θ/θ_{max} angles during the computation.

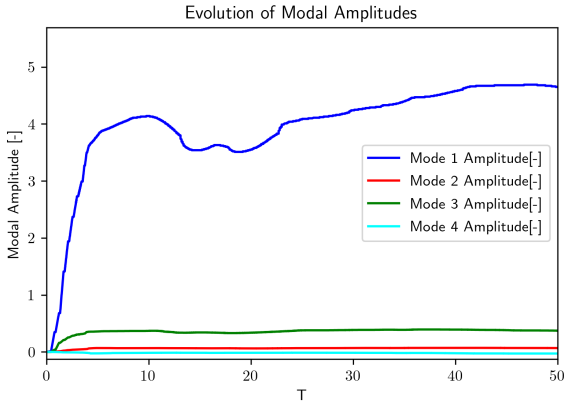

(d) Evolution of modal amplitudes during the computation.

Figure 11. Overview of the VPP results for the upwind case presented in Section 6.

REFERENCES

Abgrall, M. (2024). Adaptive Grid Refinement Procedure for RANS-based Seakeeping Computations. PhD thesis.

Böhm, C. (2014). A Velocity Prediction Procedure for Sailing Yachts with a Hydrodynamic Model Based on Integrated Fully Coupled RANSE-Free-Surface Simulations. PhD thesis. TU Delft.

Deng, G. B. et al. (2015). Verification and Validation of Resistance and Propulsion Computation. *Proceedings of Tokyo 2015 - A Workshop on Numerical Ship Hydrodynamics*. Tokyo.

Forrester, A. and Keane, A. (2009). Recent advances in surrogate-based optimization. *Prog Aerosp Sci* 45(1-3), pp. 50–79. DOI: doi:10.1016.paerosci.2008.11.001.

Gerhardt, F. C. et al. (2009). Tacking in the wind tunnel. *SNAME 19th Chesapeake Sailing Yacht Symposium*. Annapolis, Maryland, USA,

Kerdraon, P. (2021). Modeling of unsteady hydrodynamic phenomena on an offshore racing trimaran. PhD thesis. Fluid Mechanics. École centrale de Nantes.

Kjellberg, M., Gerhardt, F., and Werner, S. (2023). Sailing Performance of Wind-Powered Cargo Vessel in Unsteady Conditions. *Journal of Sailing Technology* 8, pp. 218–254.

Leroyer, A. (2004). Fluid/Motion interaction for solid and flexible bodies by resolution of the Navier-Stokes equations. Contribution to the numerical modelisation of cavitating flows. PhD thesis. Ecole Centrale de Nantes.

Leroyer, A. and Visonneau, M. (2005). Numerical Methods for RANSE Simulations of a Self-Propelled Fish-like Body. *Journal of Fluids and Structures* 20.7, pp. 975–991.

Lindstrand Levin, R. and Larsson, L. (2017). Sailing Yacht Performance Prediction Based on Coupled CFD and Rigid Body Dynamics in 6 Degrees of Freedom. *Ocean Engineering* 144, pp. 362–373.

Mouton, L. et al. (2018). Towards Unsteady Approach for Future Flutter Calculation. *Journal of Sailing Technology* 3, pp. 1–19.

ORC, Offshore Racing Congress (2021). ORC VPP Documentation 2021. `https://www.orc.org/rules/ORC`.

Persson, A., Larsson, L., and Finnsgård, C. (2021). An Improved Procedure for Strongly Coupled Prediction of Sailing Yacht Performance. *Journal of Sailing Technology* 6.01, pp. 133–150.

Prince, M. and Claughton, A. (2016). The SYRF Wide Light Project. *Proceedings of SNAME 22nd Chesapeake Sailing Yacht Symposium*. Annapolis, Maryland, USA,

Pržulj, V. and Basara, B. (2001). Bounded convection schemes for unstructured grids. *15th AIAA Computational Fluid Dynamics Conference*. AIAA paper 2001-2593. Anaheim, CA.

Queutey, P. and Visonneau, M. (2007). An Interface Capturing Method for Free-Surface Hydrodynamic Flows. *Computers & Fluids* 36.9, pp. 1481–1510.

Richeux, J. (2022). Towards the Automation of Adaptive RANS Simulations for Hydrofoils. PhD thesis.

Robin, P. et al. (2022). Starting off the Right Foot with Foil Sock Approach and AGR criterion. *Proceedings of 24th Numerical Towing Tank Symposium.* Zagreb, Croatia.

Robin, P. et al. (2024). Tackling modern sailing challenges with a CFD-based Dynamic VPP. *Journal of Sailing Technology* 9, pp. 1–18.

Roux, Y. et al. (2008). Strongly Coupled VPP and CFD RANSE Code for Sailing Yacht Performance Prediction. *Proceedings of 3rd High Performance Yacht Design Conference*. Auckland, New Zealand.

Volpi, S. et al. (2015). Development and Validation of a Dynamic Metamodel Based on Stochastic Radial Basis Functions and Uncertainty Quantification. *Structural and Multidisciplinary Optimization* 51, pp. 347–368.

Wackers, J. et al. (2011). Free-surface Viscous Flow Solution Methods for Ship Hydrodynamics. *Archives of Computational Methods in Engineering* 18, pp. 1–41.

Wackers, J. et al. (2014). Combined refinement criteria for anisotropic grid refinement in free-surface flow simulation. *Computers and Fluids* 92, pp. 209–222.

Wackers, J. et al. (2017). Can Adaptive Grid Refinement Produce Grid-Independent Solutions for Incompressible Flows? *Journal of Computational Physics* 344, pp. 364–380.

Wackers, J. et al. (2022). Adaptive Grid Refinement for Ship Resistance Computations. *Ocean Engineering* 250, p. 110969.

Wackers, J. et al. (2025). Mesh adaptation and dynamic positioning for the efficient simulation of lifting hydrofoil flows. *Ocean Engineering* 315, pp. 1–16.